

# Radiative parton energy loss and jet quenching in high-energy heavy-ion collisions \*

B.G. Zakharov

*Fakultät für Physik, Universität Bielefeld*

*D-33501 Bielefeld, Germany*

*and*

*L.D. Landau Institute for Theoretical Physics, GSP-1, 117940,*

*Kosygina Str. 2, 117334 Moscow, Russia*

## Abstract

We study within the light-cone path integral approach [3] the effect of the induced gluon radiation on high- $p_T$  hadrons in high-energy heavy-ion collisions. The induced gluon spectrum is represented in a new form which is convenient for numerical simulations. For the first time, computations are performed with a realistic parametrization of the dipole cross section. The results are in reasonable agreement with suppression of high- $p_T$  hadrons in  $Au + Au$  collisions at  $\sqrt{s} = 200$  GeV observed at RHIC.

1. One of the most interesting results obtained at RHIC is the suppression of high- $p_T$  hadrons in  $Au + Au$  collisions (for a review of the data, see [1]). It is widely believed that parton energy loss due to the induced gluon radiation caused by multiple scattering in the quark-gluon plasma (QGP) produced in the initial stage of nucleus-nucleus collisions plays a major role in this phenomenon (usually called jet quenching) [2, 3, 4, 5, 6, 7] (for a review, see [8]). The most general approach to the induced gluon emission is the light-cone path integral (LCPI) approach developed in [3] (see also [9, 10, 8]). It accurately treats the mass and finite-size effects, and applies at arbitrary strength of the Landau-Pomeranchuk-Migdal (LPM) effect [11, 12]. Other available approaches have limited domains of applicability, and can only be used either in the regime of strong (the BDMPS formalism [2, 5]) or weak (the GLV formalism [6]) LPM suppression (the GLV approach [6], in addition, is restricted to the emission of soft gluons). For this reason they can not be used for an accurate analysis of jet quenching for RHIC (and LHC) conditions.

The LCPI approach expresses the gluon spectrum through the solution of a two-dimensional Schrödinger equation with an imaginary potential in the impact parameter plane. The imaginary potential is proportional to the cross section of interaction of the  $\bar{q}qg$  system (for  $q \rightarrow gq$  transition) with a particle in the medium,  $\sigma_3(\rho)$  (here  $\rho$  is the transverse distance between quark and gluon, the antiquark is located at the center of mass of the  $qg$ -system). The  $\sigma_3(\rho)$  can be written as  $\sigma_3(\rho) = C(\rho)\rho^2$ . The factor  $C(\rho)$  has a smooth (logarithmic) dependence on  $\rho$  for  $\rho \ll 1/\mu_D$  (hereafter,  $\mu_D$  is the Debye

---

\*Supported by DFG-grant Schi 189/6-1

screening mass). If one replaces  $C(\rho)$  by  $C(\rho_{eff})$ , where  $\rho_{eff}$  is the typical value of  $\rho$ , the Hamiltonian takes the oscillator form. This approximation, which greatly simplifies the calculations, was employed in several analyses [4, 7, 13] (it was also used in the BDMPS approach [2, 5]). However, the oscillator approximation turns out to be too crude and unsatisfactory. First of all, for RHIC and LHC conditions, the dominating  $\rho$  scale is not small enough and the results depend strongly on the choice of  $\rho_{eff}$ . Another reason why the oscillator approximation is unsatisfactory is more serious. In the high energy limit the gluon formation length,  $L_f$ , becomes larger than the quark pathlength in the QGP, and finite-size effects become important. In this regime  $\rho_{eff} \ll 1/\mu_D$ , and one might naively expect that the oscillator approximation should work very well. However, one can show [14] that in this regime the dominating  $N = 1$  rescattering contribution (and any odd rescattering) evaluated in the oscillator approximation simply vanishes. For RHIC and LHC conditions, the finite-size effects play a very important role and the oscillator approximation can lead to uncontrolled errors. For this reason, one has to use an accurate parametrization of the three-body cross section. It requires numerical calculations for solving the Schrödinger equation.

In the present paper we represent the induced gluon spectrum in a new form which is convenient for numerical computations. We, for the first time, calculate the induced gluon emission and the nuclear modification factor for RHIC conditions using a realistic imaginary potential.

**2.** We consider a quark with energy  $E$  produced in a medium at  $z = 0$  (we chose the  $z$ -axis along the quark momentum). The induced gluon spectrum in the gluon fractional longitudinal momentum  $x$  reads [3]

$$\frac{dP}{dx} = 2\text{Re} \int_0^\infty dz_1 \int_{z_1}^\infty dz_2 g(x) [K(z_2, \boldsymbol{\rho}_2 | z_1, \boldsymbol{\rho}_1) - K_v(z_2, \boldsymbol{\rho}_2 | z_1, \boldsymbol{\rho}_1)] \Big|_{\boldsymbol{\rho}_1 = \boldsymbol{\rho}_2 = 0}. \quad (1)$$

Here  $K$  is the Green's function for the Hamiltonian (acting in the transverse plane)

$$H = -\frac{1}{2M(x)} \left( \frac{\partial}{\partial \boldsymbol{\rho}} \right)^2 + v(\boldsymbol{\rho}, z) + \frac{1}{L_f}, \quad (2)$$

$$v(\boldsymbol{\rho}, z) = -i \frac{n(z) \sigma_3(\boldsymbol{\rho})}{2}, \quad (3)$$

and

$$K_v(z_2, \boldsymbol{\rho}_2 | z_1, \boldsymbol{\rho}_1) = \frac{M(x)}{2\pi i(z_2 - z_1)} \exp \left[ \frac{iM(x)(\boldsymbol{\rho}_2 - \boldsymbol{\rho}_1)^2}{2(z_2 - z_1)} - \frac{i(z_2 - z_1)}{L_f} \right] \quad (4)$$

is the Green's function for the Hamiltonian (2) with  $v(\boldsymbol{\rho}, z) = 0$ . In (2), the Schrödinger mass is  $M(x) = Ex(1-x)$ ,  $L_f = 2Ex(1-x)/[m_q^2 x^2 + m_g^2(1-x)]$  is the gluon formation length, here  $m_q$  and  $m_g$  are the quark and gluon masses that play the role of the infrared cutoffs at  $x \sim 1$  and  $x \sim 0$  (in the QGP  $m_{q,g}$  are given by the quark and gluon quasiparticle masses). In (3),  $n(z)$  is the number density of QGP, and  $\sigma_3$  is the above mentioned cross section of the color singlet  $q\bar{q}g$  system with a particle in the medium. Summation over triplet (quark) and octet (gluon) color states is implicit in (3). The  $\sigma_3$  may depend on  $z$

(through the Debye screening mass), however, below we will use  $z$ -independent  $\mu_D$ . The vertex factor  $g(x)$ , entering (1), reads

$$g(x) = \frac{\alpha_s P(x)}{2M^2(x)} \frac{\partial}{\partial \boldsymbol{\rho}_1} \cdot \frac{\partial}{\partial \boldsymbol{\rho}_2}, \quad (5)$$

where  $P(x) = C_F[1 + (1-x)^2]/x$  is the splitting function for the  $q \rightarrow gq$  transition ( $C_F$  is the quark Casimir factor). Note that we neglect the spin-flip  $q \rightarrow qq$  transition, which gives a small contribution to the quark energy loss.

The three-body cross section entering the potential (3) can be written as [15, 3]

$$\sigma_3(\rho) = \frac{9}{8} [\sigma_{q\bar{q}}(\rho) + \sigma_{q\bar{q}}((1-x)\rho)] - \frac{1}{8} \sigma_{q\bar{q}}(x\rho), \quad (6)$$

where

$$\sigma_{q\bar{q}}(\rho) = \alpha_s^2 C_T C_F \int d\mathbf{q} \frac{[1 - \exp(i\mathbf{q}\boldsymbol{\rho})]}{(q^2 + \mu_D^2)^2} \quad (7)$$

is the dipole cross section for the color singlet  $q\bar{q}$  pair ( $C_T$  is the color Casimir for the thermal parton (quark or gluon)).

The spectrum (1) can be rewritten as ( $L$  is the quark pathlength in the medium)

$$\frac{dP}{dx} = \int_0^L dz n(z) \frac{d\sigma_{eff}^{BH}(x, z)}{dx}, \quad (8)$$

$$\frac{d\sigma_{eff}^{BH}(x, z)}{dx} = \text{Re} \int_0^z dz_1 \int_z^\infty dz_2 \int d\boldsymbol{\rho} g(x) K_\nu(z_2, \boldsymbol{\rho}_2 | z, \boldsymbol{\rho}) \sigma_3(\rho) K(z, \boldsymbol{\rho} | z_1, \boldsymbol{\rho}_1) \Big|_{\boldsymbol{\rho}_1 = \boldsymbol{\rho}_2 = 0}. \quad (9)$$

$d\sigma_{eff}^{BH}/dx$  (9) can be viewed as an effective Bethe-Heitler cross section, which accounts for the LPM and finite-size effects. One can represent (9) as

$$\frac{d\sigma_{eff}^{BH}(x, z)}{dx} = -\frac{\alpha_s P(x)}{\pi M(x)} \text{Im} \int_0^z d\xi \frac{\partial}{\partial \rho} \left( \frac{F(\xi, \rho)}{\sqrt{\rho}} \right) \Big|_{\rho=0}, \quad (10)$$

where the function  $F$  is the solution to the radial Schrödinger equation for the azimuthal quantum number  $m = 1$

$$i \frac{\partial F(\xi, \rho)}{\partial \xi} = \left[ -\frac{1}{2M(x)} \left( \frac{\partial}{\partial \rho} \right)^2 - i \frac{n(z-\xi)\sigma_3(\rho)}{2} + \frac{4m^2 - 1}{8M(x)\rho^2} + \frac{1}{L_f} \right] F(\xi, \rho). \quad (11)$$

The boundary condition for  $F(\xi, \rho)$  reads  $F(\xi = 0, \rho) = \sqrt{\rho} \sigma_3(\rho) \epsilon K_1(\epsilon \rho)$ , where  $\epsilon = [m_q^2 x^2 + m_g^2 (1-x)^2]^{1/2}$ , and  $K_1$  is the Bessel function. In deriving (10), we used the relations [9]

$$\frac{\partial}{\partial \boldsymbol{\rho}_1} \cdot \frac{\partial}{\partial \boldsymbol{\rho}_2} = \frac{1}{2} \left[ \left( \frac{\partial}{\partial x_1} - i \frac{\partial}{\partial y_1} \right) \cdot \left( \frac{\partial}{\partial x_2} + i \frac{\partial}{\partial y_2} \right) + \left( \frac{\partial}{\partial x_1} + i \frac{\partial}{\partial y_1} \right) \cdot \left( \frac{\partial}{\partial x_2} - i \frac{\partial}{\partial y_2} \right) \right],$$

$$\left( \frac{\partial}{\partial x_2} \pm i \frac{\partial}{\partial y_2} \right) \int_z^\infty dz_2 K_v(z_2, \boldsymbol{\rho}_2 | z, \boldsymbol{\rho}) \Big|_{\boldsymbol{\rho}_2=0} = \pm \frac{M(x)}{i\pi} \exp(\pm i\phi) K_1(\epsilon\rho).$$

The time variable  $\xi$  in (10), in terms of the variables  $z$  and  $z_1$  of equation (9), is given by  $\xi = z - z_1$ ; i.e., contrary to the Schrödinger equation for the Green's functions entering (1), (10) represents the spectrum through the solution to the Schrödinger equation, which describes evolution of the  $q\bar{q}g$  system back in time. It allows one to have a smooth boundary condition, which is convenient for numerical calculations.

**3.** The jet quenching is usually characterized by the nuclear modification factor (we consider the central rapidity region  $y \sim 0$  and suppress the explicit  $y$ -dependence)

$$R_{AA}(p_T) = \frac{d\sigma^{AA}(p_T)/dydp_T^2}{N_{bin}d\sigma^{pp}(p_T)/dydp_T^2}, \quad (12)$$

where  $d\sigma^{AA}/dydp_T^2$  and  $d\sigma^{pp}/dydp_T^2$  are the inclusive cross section for  $A + A$  and  $p + p$  collisions, and  $N_{bin}$  is the number of the binary nucleon-nucleon collisions. The effect of the parton energy loss on the high- $p_T$  hadron production in  $A + A$  collisions can approximately be described in terms of effective hard partonic cross sections, which account for the induced gluon emission [16]. Using the power-law parametrization for cross section of quark production in  $p + p$  collisions  $\propto 1/p_T^{n(p_T)}$  one can obtain

$$R_{AA}(p_T) \approx P_0(p_T) + \frac{1}{J(p_T)} \int_0^1 dz z^{n(p_T)-2} D_q^h(z, \frac{p_T}{z}) \int_0^1 dx (1-x)^{n(p_T/z)-2} \frac{dI(x, \frac{p_T}{z(1-x)})}{dx}, \quad (13)$$

$$J(p_T) = \int_0^1 dz z^{n(p_T)-2} D_q^h(z, \frac{p_T}{z}), \quad (14)$$

where  $P_0$  is the probability of quark propagation without induced gluon emission,  $dI(x, p_T)/dx$  is the probability distribution in the quark energy loss for a quark with  $E = p_T$ ,  $D_q^h(z, p_T/z)$  is the quark fragmentation function. Note that, since  $n(p_T) \gg 1$ , the  $z$ -integrands in (13), (14) are sharply peaked at  $z \approx \bar{z}$  ( $\bar{z}$  is the value of  $z$  at which  $z^{n(p_T)-2} D_q^h(z, p_T/z)$  has a maximum). For this reason (13) to quite good accuracy can be approximated as

$$R_{AA}(p_T) \approx P_0(p_T) + \int_0^1 dx (1-x)^{n(p_T/\bar{z})-2} \frac{dI(x, \frac{p_T}{\bar{z}(1-x)})}{dx}. \quad (15)$$

We take the  $P_0$  and spectrum in the radiated energy entering (13) in the form

$$P_0(E) = \exp\left(-\int_{x_{min}}^1 dx \frac{dP(x, E)}{dx}\right), \quad (16)$$

$$\frac{dI(x, E)}{dx} = \frac{dP(x, E)}{dx} \cdot \exp\left(-\int_x^1 dy \frac{dP(y, E)}{dy}\right), \quad (17)$$

where  $x_{min} \approx m_g/E$ , and it is assumed that the spectrum equals zero at  $x \leq x_{min}$ . Formula (17) corresponds to the leading order term of the series in  $L/L_{rad}$  (here  $L_{rad}$  is the radiation length corresponding to the energy loss  $\Delta E \sim E$ ) of the spectrum derived in [17] for the photon emission and, strictly speaking, is only valid for  $\Delta E \ll E$ . However, even for the more broad domain  $\Delta E \lesssim E$  (which is interesting from the point of view of jet quenching at RHIC) (17) reproduces the energy loss spectrum evaluated assuming independent gluon radiation to a reasonable accuracy. An accurate calculation of the nuclear modification factor accounting for the higher order terms in  $L/L_{rad}$  in the approximation of independent gluon emission [16] does not make sense because this approximation itself does not have any theoretical justification. Note that our spectrum is automatically normalized to unity.

The effective exponent  $n(p_T)$  for quark production entering (13) is close to that for hadron production,  $n_h(p_T)$ . A small difference between these quantities (stemming from the  $p_T$  dependence of the integral (14)) is given by  $n(p_T) - n_h(p_T) = d \ln J(p_T)/d \ln p_T$ . For  $Au + Au$  collisions at  $\sqrt{s} = 200$  GeV we use  $n_h(p_T) = np_T/(p_T + b)$  with  $n = 9.99$  and  $b = 1.219$  corresponding to the parametrization  $d\sigma/dydp_T^2 = A/(p_T + b)^n$  obtained in [18] for  $\pi^0$  production in  $p + p$  collisions. The above procedure allows one to avoid uncertainties of the pQCD calculations of the partonic cross sections.

4. To fix the  $m_{q,g}$  and  $\mu_D$  we use the results of the analysis of the lattice calculations within the quasiparticle model [19]. For the relevant range of temperature of the plasma  $T \sim (1 - 3)T_c$  ( $T_c \approx 170$  MeV is the temperature of the deconfinement phase transition) the analysis [19] gives for the quark and gluon quasiparticle masses  $m_q \approx 0.3$  and  $m_g \approx 0.4$  GeV. With the above value of  $m_g$  from the perturbative relation  $\mu_D = \sqrt{2}m_g$  one obtains  $\mu_D \approx 0.57$  GeV. To study the infrared sensitivity of our results we also perform computations for  $m_g = 0.75$  GeV (with  $\mu_D = 0.57$  GeV). This value of the infrared cutoff for gluon emission in parton-nucleon interaction has been obtained from the analysis of the low- $x$  proton structure function within the dipole BFKL equation [15, 20]. It seems to be reasonable for gluon emission in the developed mixed phase and for fast gluons with  $L_f \gtrsim L$ . This value agrees well with the natural infrared cutoff for gluon emission in the vacuum  $m_g \sim 1/R_c$ , where  $R_c \approx 0.27$  fm is the gluon correlation radius in the QCD vacuum [21]. The above two values of  $m_g$  give reasonable lower and upper limits of the infrared cutoff for the induced gluon emission for RHIC and LHC conditions.

We perform numerical calculations for fixed and running  $\alpha_s$ . In the first case we take  $\alpha_s = 0.5$  for gluon emission from light quarks and gluons, and  $\alpha_s = 0.4$  for the case of  $c$ -quark. For the running  $\alpha_s$ , we use the parametrization (with  $\Lambda_{QCD} = 0.3$  GeV) frozen at  $\alpha_s = 0.7$  at low momenta. This parametrization is consistent with the integral of  $\alpha_s(Q)$  in the interval  $0 < Q < 2$  GeV obtained from the analysis of the heavy quark energy loss (in vacuum) [22]. Previously this parametrization was used to describe successfully the HERA data on the low- $x$  proton structure function within the dipole BFKL approach [15, 20]. To incorporate the running  $\alpha_s$  in our formalism, we include  $\alpha_s$  in the integrand on the right-hand side of (10) and take for virtuality  $Q^2 = aM(x)/\xi$ . The parameter  $a$  was adjusted to reproduce the  $N = 1$  rescattering contribution evaluated in the ordinary diagrammatic approach [23]. It gives  $a \approx 1.85$ . For the dipole cross section (7) we take  $Q^2 = \mathbf{q}^2$ .

We assume the Bjorken [24] longitudinal expansion of the QGP with  $T^3\tau = T_0^3\tau_0$  which gives  $n(z) \propto 1/z$  for  $z > \tau_0$ . We use the initial conditions suggested in [25]:  $T_0 = 446$  MeV and  $\tau_0 = 0.147$  fm for RHIC, and  $T_0 = 897$  MeV and  $\tau_0 = 0.073$  fm for LHC. For RHIC, the above condition were obtained from the charged particle pseudorapidity density  $dN/dy \approx 1260$  measured by the PHOBOS experiment [26] in  $Au + Au$  collisions at  $\sqrt{s} = 200$  GeV assuming an isentropic expansion and rapid thermalization at  $\tau_0 \sim 1/3T_0$ . The LHC parameters correspond to  $dN/dy \approx 5625$  at  $\sqrt{s} = 5.5$  TeV, which was estimated in [27]. The above initial conditions for RHIC (translated into  $\tau_0 = 0.6$  fm) agree with those used in successful hydrodynamic description of  $Au + Au$  collisions at RHIC [28]. Note that, since the dominating  $\rho$ -scale in (9)  $\propto \sqrt{z}$  for  $z \ll L_f$ , our results are not very sensitive to  $\tau_0$  (for a given entropy). The maximum parton pathlength in the hot QCD medium is restricted by the life-time of the QGP (and mixed) phase,  $\tau_{max}$ .<sup>1</sup> We take  $\tau_{max} \sim R_A \sim 6$  fm. This seems to be a reasonable value for central heavy-ion collisions, since, due to the transverse expansion, the hot QCD matter should cool quickly at  $\tau \gtrsim R_A$  [24].

In Fig. 1 we show the induced gluon spectrum for  $q \rightarrow gq$  transition for RHIC conditions for the quark pathlength  $L = 6$  fm obtained with  $m_q = 0.3$  and  $m_q = 1.5$  GeV for  $m_g = 0.4$  and  $m_g = 0.75$  GeV. In Fig. 1 we also show the Bethe-Heitler spectrum (dashed line). One sees that the LPM and finite-size effects strongly suppress the gluon emission. The gluon emission from  $c$ -quark is suppressed in comparison with light quark due to larger mass, which leads to decreasing of the dominating  $\rho$  scale (note that the spectrum is not sensitive to the light quark mass, except for  $x \sim 1$ ). One can see from Fig. 1 that, although the Bethe-Heitler spectrum differs strongly for two values of  $m_g$ , the difference becomes relatively small for the spectrum, which accounts for the LPM and finite-size effects. It is connected with the fact that, due to the multiple scattering and finite-size effects, the dominating  $1/\rho$ -scale becomes larger than  $m_g$ ; namely this in-medium scale plays the role of the infrared cutoff at high energies [4] (however, of course, for not very high  $p_T$  the value of  $m_g$  is still important). We do not show the spectra for running  $\alpha_s$ . They are similar in form (but somewhat suppressed at moderate fractional momenta). The LPM suppression for LHC is considerably stronger than for RHIC, but the spectra are similar in form, and we do not show them as well.

In Fig. 2 we plot the quark energy loss  $\Delta E = E \int_{x_{min}}^1 dx x dP/dx$  evaluated for fixed (solid line) and running (dashed line)  $\alpha_s$  for RHIC and LHC conditions for  $L = 6$  fm with  $m_g = 0.4$  GeV (thick lines) and  $m_g = 0.75$  GeV (thin lines). The results for  $\alpha_s = 0.5$  agree roughly with that for running  $\alpha_s$  for  $E \lesssim 10$  GeV but at higher energies the energy dependence is steeper for fixed  $\alpha_s$ . This says that the typical  $\rho$ -scale becomes smaller with increasing energy. It is also seen from the decrease of the relative difference between the curves for  $m_g = 0.4$  and  $0.75$  GeV.

In Fig. 3a we compare the nuclear modification factor (13) for  $T_0 = 446$  MeV calculated using the NLO KKP fragmentation functions [29] for running  $\alpha_s$  with that obtained at RHIC [1] for central  $Au + Au$  collisions at  $\sqrt{s} = 200$  GeV. For illustration of the

---

<sup>1</sup>For our choice of the initial conditions the life-time of QGP is  $\sim 3$  fm for RHIC. However, in the interval  $\tau \sim 3 - 6$  fm the density of the mixed phase is practically the same as that for the pure QGP phase.

dependence on  $T_0$ , in Fig. 3b we also present the results for  $T_0 = 375$  MeV. The theoretical curves were obtained for  $L = 4.9$  fm. It is the typical parton pathlength in the QGP (and mixed) phase for  $\tau_{max} = 6$  fm. We present the results for  $m_g = 0.4$  and  $0.75$  GeV. For  $p_T \lesssim 15$  the results for  $\alpha_s = 0.5$  are close to that for running  $\alpha_s$  and we do not plot them. The results for the quark (solid line) and gluon (dashed line) jets are shown separately (note that for  $\sqrt{s} = 200$  GeV the quark and gluon contributions are comparable). The suppression is somewhat stronger for gluon jets. One can see from Fig. 3a that the theoretical  $R_{AA}$  for  $m_g = 0.4$  is in reasonable agreement with the experimental one. One should bear in mind, however, that our calculations neglect the collisional energy loss [30]. For  $p_T \sim 5 - 15$  GeV the collisional energy loss may increase the total energy loss by  $\sim 30 - 40\%$ . In this case (if one takes the initial conditions [25]) the value  $m_g = 0.75$  GeV would be more preferable for agreement with the RHIC data. As mentioned previously, this value is reasonable for the mixed phase and for gluons with  $L_f \gtrsim L$ . Since, for  $\sqrt{s} = 200$  GeV, the medium spends about half of its time in the mixed phase, the effective infrared cutoff may be larger than the gluon quasiparticle mass in the QGP. For this reason, the collisional energy loss may be included without using an unrealistic infrared cutoff for the induced energy loss. The possible remaining small disagreement with the data may be avoided by taking a somewhat smaller value of  $T_0$  (or  $\alpha_s$ ). In any case, it is clear that, for such a complicated phenomenon, it is hardly possible to expect a perfect agreement with experiment and the agreement found in the present paper is surprisingly good.

The above estimate for the collisional energy loss has been obtained for the pQCD plasma. Presently, there are some indications [31] that the medium produced at RHIC may be a strongly coupled QGP. The radiative energy loss should not be very sensitive to the dynamics of the QGP (for the same number density of the QGP). However, it may be important for the collisional energy loss. Unfortunately, the corresponding calculations have not been made yet. It is interesting that our results give support for the scenario with strongly coupled QGP. Indeed, this scenario requires  $\alpha_s \gtrsim 0.5$  [31] for thermal partons. The  $R_{AA}$  is sensitive to the radiation of soft gluons with an energy of about a few  $\mu_D$ . One can expect that, for such gluons,  $\alpha_s$  should be close to that for thermal partons. We obtained agreement with the data with  $\alpha_s$ , which is frozen at a value of  $0.7$  at low momenta. If  $\alpha_s$  is frozen at a value below  $0.4-0.5$ , the theoretical  $R_{AA}$  strongly disagrees with that observed at RHIC.

**5.** In summary, we have represented, within the LCPI approach [3], the induced gluon spectrum in a new form convenient for numerical calculations and carried out computations of the induced gluon emission from fast partons in the expanding QGP for RHIC and LHC conditions. The calculations for, the first time, have been performed with a realistic parametrization of the dipole cross section. The theoretical nuclear modification factor calculated for the initial conditions obtained from the charged particle rapidity density observed at RHIC [25] and the hydrodynamic simulation of the RHIC data [28] is in a reasonable agreement with that observed at RHIC.

**Acknowledgements.** I thank R. Baier and D. Schildknecht for discussions and their kind hospitality at the University of Bielefeld, where this work was completed. I am also grateful to the High Energy Group of the ICTP for their kind hospitality during my visit

to Trieste, where part of this work was done.

## References

- [1] D. d'Enterria, Invited overview talk at 39th Rencontres de Moriond on QCD and High-Energy Hadronic Interactions, La Thuile, Italy, 28 Mar - 4 Apr 2004; nucl-ex/0406012.
- [2] R. Baier, Y.L. Dokshitzer, A.H. Mueller, S. Peigné and D. Schiff, Nucl. Phys. B**483**, 291 (1997); *ibid.* B**484**, 265 (197).
- [3] B.G. Zakharov, JETP Lett. **63**, 952 (1996).
- [4] B.G. Zakharov, JETP Lett. **65**, 615 (1997).
- [5] R. Baier, Y.L. Dokshitzer, A.H. Mueller and D. Schiff, Nucl. Phys. B**531**, 403 (1998).
- [6] M. Gyulassy, P. Lévai and I. Vitev, Nucl. Phys. B**594**, 371 (2001).
- [7] U.A. Wiedemann, Nucl. Phys. A**690**, 731 (2001).
- [8] R. Baier, D. Schiff and B.G. Zakharov, Ann. Rev. Nucl. Part. **50**, 37 (2000).
- [9] B.G. Zakharov, Phys. Atom. Nucl. **61**, 838 (1998).
- [10] B.G. Zakharov, JETP Lett. **70**, 176 (1999).
- [11] L.D. Landau and I.Ya. Pomeranchuk, Dokl. Akad. Nauk SSSR **92**, 535, 735 (1953).
- [12] A.B. Migdal, Phys. Rev. **103**, 1811 (1956).
- [13] C.A. Salgado and U.A. Wiedemann, Phys. Rev. Lett. **89**. 092303 (2002); C.A. Salgado and U.A. Wiedemann, Phys. Rev. D **68**, 014008 (2003).
- [14] B.G. Zakharov, JETP Lett. **73**, 49 (2001).
- [15] N.N. Nikolaev, B.G. Zakharov and V.R. Zoller, Phys. Lett. B**328**, 486 (1994).
- [16] R. Baier, Yu.L. Dokshitzer, A.H. Mueller and D. Schiff, JHEP **0109**, 033 (2001); hep-ph/0106347 (2001).
- [17] B.G. Zakharov, Phys. Atom. Nucl. **62**, 1008 (1999); JETP Lett. **78**, 759 (2003).
- [18] S.S. Adler *et al.* [PHENIX Collaboration], Phys. Rev. Lett. **91**, 241803 (2003).
- [19] P. Lévai and U. Heinz, Phys. Rev. C**57**, 1879 (1998).
- [20] N.N. Nikolaev and B.G. Zakharov, Phys. Lett. B**327**, 149 (1994).
- [21] E.V. Shuryak, Rev. Mod. Phys. **65**, 1 (1993).



- [22] Yu.L. Dokshitzer, V.A. Khoze and S.I. Troyan, Phys. Rev. D**53**, 89 (1996).
- [23] B.G. Zakharov, JETP Lett. **80**, 67 (2004).
- [24] J.D. Bjorken, Phys. Rev. D**27**, 140 (1983).
- [25] R.J. Fries, B. Müller and D.K. Srivastava, Phys. Rev. Lett. **90**, 132301 (2003).
- [26] B.B. Back *et al.* [PHOBOS Collaboration], Phys. Rev. C**65**, 061901 (2002).
- [27] J. Kapusta, L.D. McLerran and D.K. Srivastava, Phys. Lett. B**283**, 145 (1992).
- [28] U. W. Heinz and P. F. Kolb, Nucl. Phys. A**702**, 269 (2002).
- [29] B. A. Kniehl, G. Kramer and B. Potter, Nucl. Phys. B**582**, 514 (2000).
- [30] J.D. Bjorken, Fermilab preprint Pub-82/59-THY (1982).
- [31] E.V. Shuryak, hep-ph/0405066; E.V. Shuryak and I. Zahed, hep-ph/0403127.

## Figures

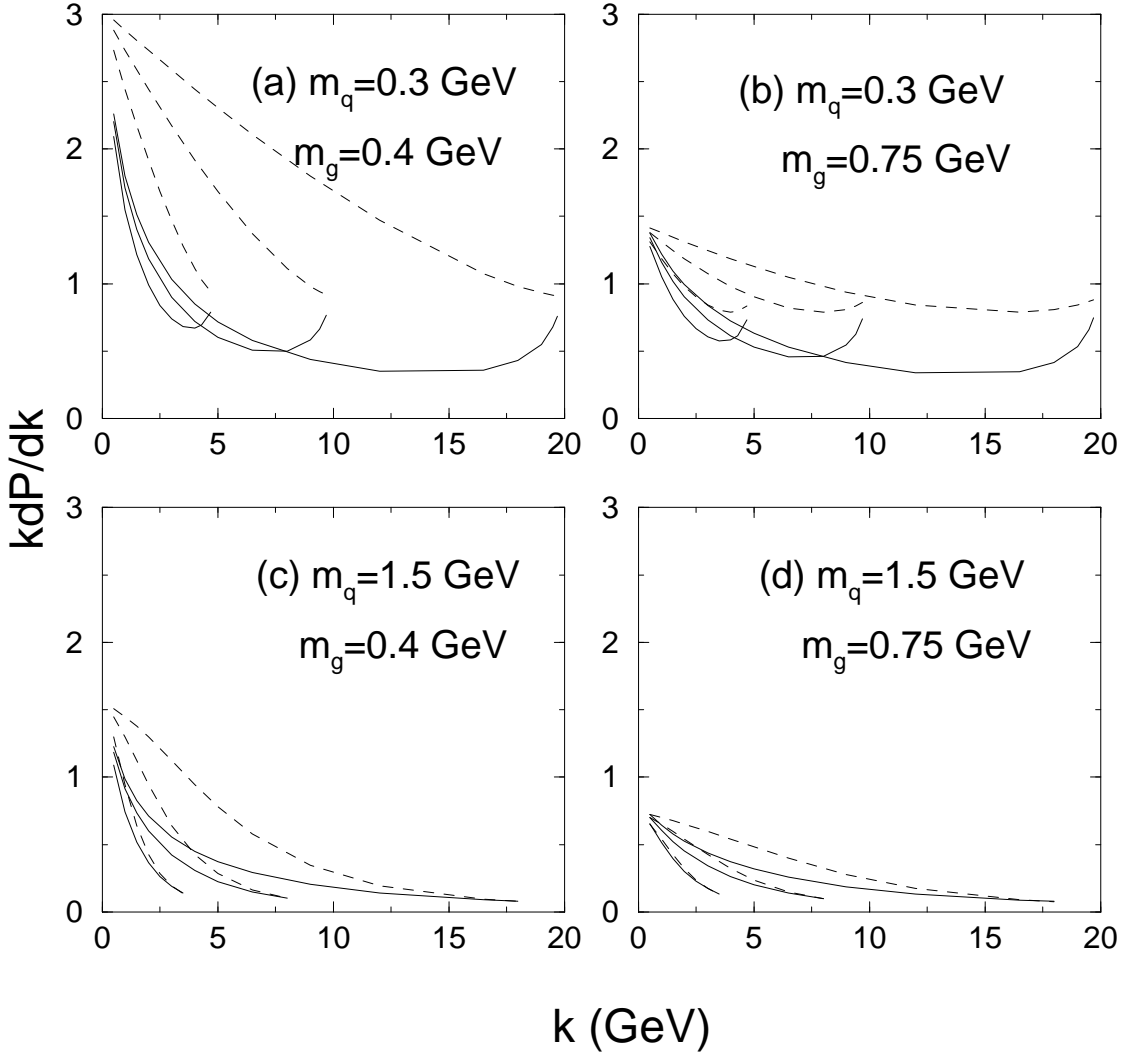


Figure 1: The induced gluon spectrum (solid line) for  $q \rightarrow gq$  transition versus the gluon momentum  $k$  for RHIC conditions for  $E = 5, 10$  and  $20$  GeV,  $L = 6$  fm obtained using (8), (10) with  $\alpha_s = 0.5$  for  $m_q = 0.3$  GeV (a,b) and  $m_q = 1.5$  GeV (c,d);  $m_g = 0.4$  GeV (left) and  $0.75$  GeV (right). The Bethe-Heitler spectrum is shown by the dashed line.

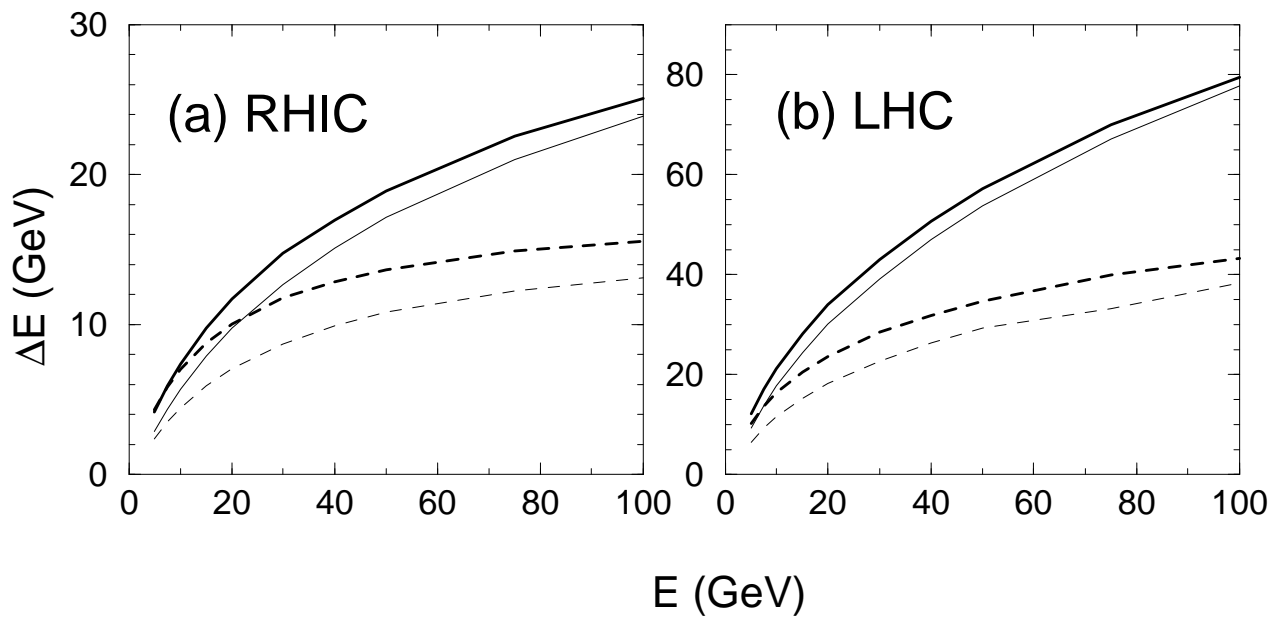


Figure 2: The energy dependence of the quark energy loss for RHIC (a) and LHC (b) for  $L = 6$  fm obtained with  $\alpha_s = 0.5$  (solid line) and running  $\alpha_s$  (dashed line),  $m_g = 0.4$  GeV (thick lines) and  $m_g = 0.75$  GeV (thin lines),  $m_q = 0.3$  GeV.

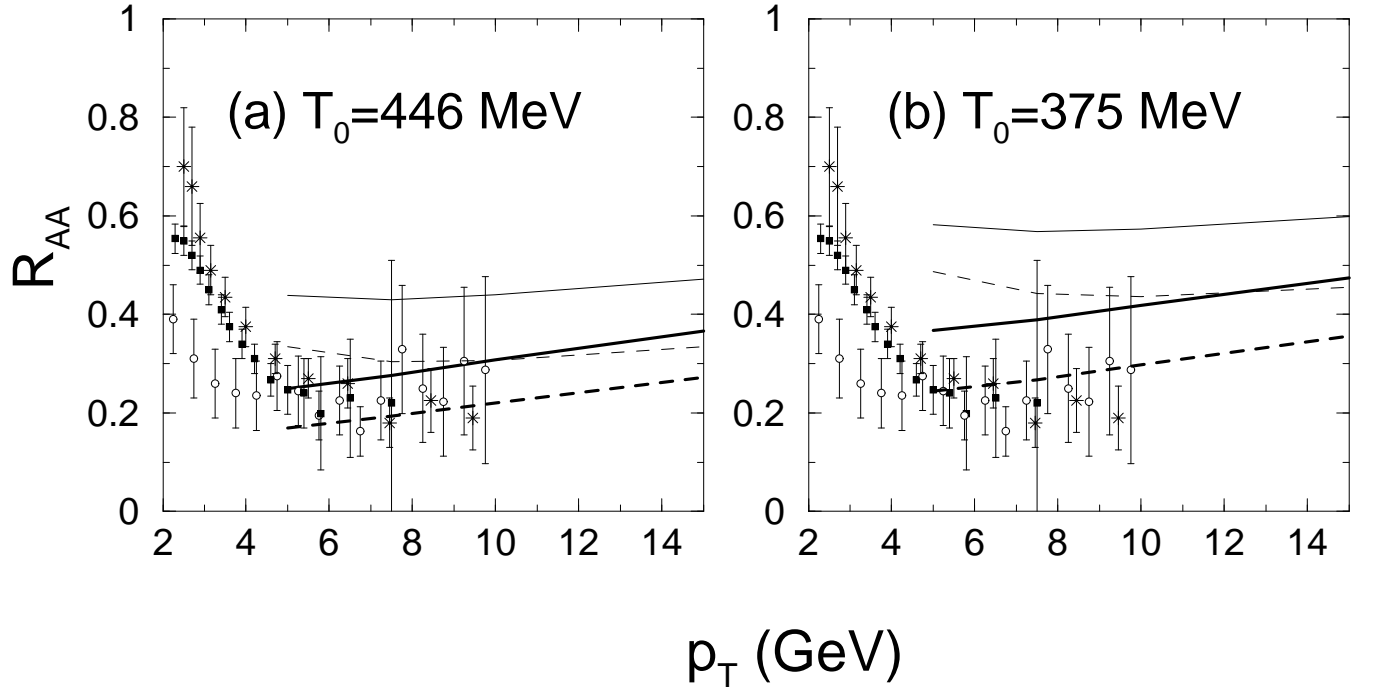


Figure 3: The nuclear modification factor (13) for central  $Au + Au$  collisions at  $\sqrt{s} = 200$  GeV for quark (solid line) and gluon (dashed line) jets obtained with  $m_g = 0.4$  GeV (thick lines) and  $m_g = 0.75$  GeV (thin lines) for running  $\alpha_s$ . The experimental points (from [1]) are for the following: circle -  $Au + Au \rightarrow \pi^0 + X$  (0-10% central) [PHENIX Collaboration], square -  $Au + Au \rightarrow h^\pm + X$  (0-10% central) [PHENIX Collaboration], star -  $Au + Au \rightarrow h^\pm + X$  (0-5% central) [STAR Collaboration].